

# Selective Soldering on Printed Circuit Boards with Endogenous Induction Heat at Appropriate Susceptors

Dirk Seehase<sup>1\*</sup>, Christian Kohlen<sup>1</sup>, Arne Neiser<sup>2</sup>, Andrej Novikov<sup>1</sup>, Mathias Nowottnick<sup>1</sup>

<sup>1</sup> Institute of Electronic Appliances and Circuits, Faculty of Computer Science and Electrical Engineering, University of Rostock, Albert-Einstein-Str. 2, 18059 Rostock, Germany

<sup>2</sup> Seho Systems GmbH, Frankenstraße 7-11, Kreuzwertheim, Germany

\* Corresponding author, e-mail: [dirk.seehase@uni-rostock.de](mailto:dirk.seehase@uni-rostock.de)

Received: 10 October 2018, Accepted: 07 November 2018, Published online: 30 November 2018

## Abstract

In this work, methods for the endogenous heating of printed circuit boards (PCBs) by means of inductive losses in built-in susceptors are presented. Two basic types of inductive heating were studied, the heating in the transversal field and the heating in the longitudinal field. Elementary test stands were constructed and characterized for both field geometries. These setups were then used to analyze various susceptor materials like copper and aluminum for the transversal field heating and nickel and iron for the longitudinal field heating. To demonstrate the soldering processes by means of inductive heating, exemplary processes were conducted on both test stands by emulating a standard solder reflow profile. The limitations of using induction heating on printed circuit boards are illustrated by component lead frames, which also heat up in the inductive field and can hence be damaged.

In short, this paper presents a selective heating method, based on induction heating, for printed circuit boards. Furthermore possible setups for implementing this heating method are described.

## Keywords

PCB, induction, heating, soldering, susceptor

## 1 Introduction

Reflow soldering methods used today often offer no possibility of local or selective heating of individual components. Also the heat transfer mechanism which is primarily used by the industry is convection, which only has a low heat transfer coefficient. An exception to this is vapor phase soldering (VPS), in which a fluid condensing on the assembly transfers its temperature via heat conduction with a much higher coefficient [1]. Due to the self-contained process chamber, VPS is more difficult to incorporate in industrial production lines.

If components of different thermal masses are to be soldered within a typical convection reflow system on the same board, problems can therefore arise. While large isolated components, such as BGAs, heat up significantly more slowly, the majority of the rest of the assembly is made up of small passive components that quickly assume the process temperature. This behavior is illustrated in Fig. 1 with a thermal simulation and a thermal measurement at a PCB being convectively reflowed.

Also, a simulation for the difference in convective heating of a small and large solder deposit is presented in [2].

One way of compensating for this difference could be to support soldering by inductive heating. Thus used, an appropriate susceptor then represents an embedded heating structure within a PCB. Similar studies have been made in [3-5], where embedded heating elements were realized by a resistive layer, at which Joule heating occurs through a DC voltage drop. The basic principle for this process is depicted in Fig. 2.

In this work, an approach for inductive heating of a PCB shall be pursued. For this purpose, a suitably positioned susceptor is placed below or within the substrate near the area to be heated. If the susceptor is exposed to an alternating magnetic field generated by specially designed inductor coils, the various loss mechanisms (hysteresis losses, eddy current losses and excess losses [6]) cause the material to heat up (Fig. 3). By heat conduction of the process heat to the solder joint, a melting of the solder can take place.

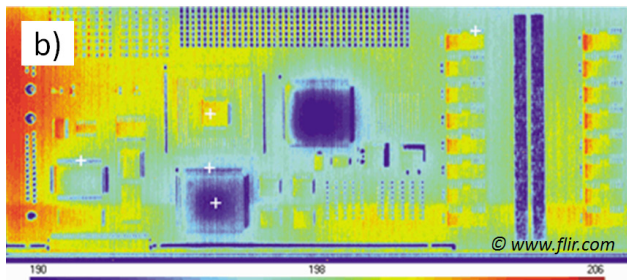
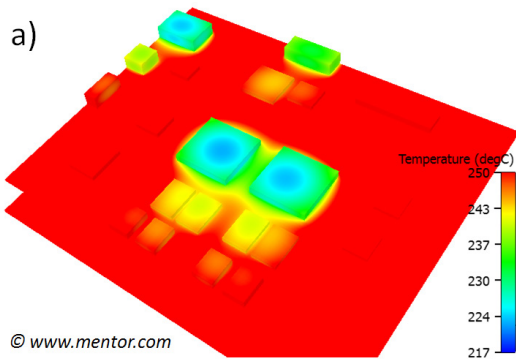


**Fig. 1** Temperature distribution during reflow soldering of printed circuit boards; a) simulated with FloTHERM®; b) measured with in-line thermal imaging.

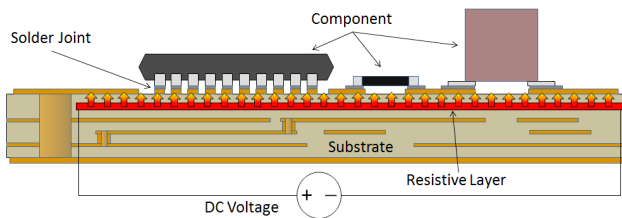


**Fig. 2** Heating of solder joints with ohmic heat generated on an embedded resistive layer.

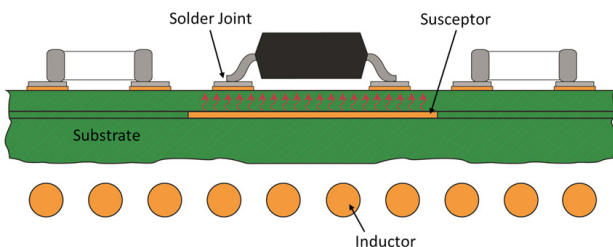


**Fig. 3** Heating of a solder joint with inductively generated heat on an embedded susceptor.

Compared to the approach of heating with a resistive layer inside the substrate, the induction process offers the possibility of non-contact between the sample to be heated and the surrounding machinery. The inductive coupling between exciter (coil) and consumer (susceptor)

allows for a wireless energy transfer, whereas Joule heating requires supply and return wiring as a galvanic coupling between the embedded heating layer and the external power source. Nevertheless, it should be noted at this point that the system requirements for heating with a controlled induction field are much more demanding.

In the electrical industry inductive heating methods are common, especially for brazing and soldering. In most cases, this involves the joining of electromechanical components, which must be soldered selectively and outside the standard soldering process.

Such selective soldering applications are presented for example in [7-9]. In these, the induction heat is generated either at the component terminals or directly within the solder material. Another possibility to increase the efficiency of heating or to work with other field parameters is discussed in [10]. Here, FeCo nanoparticles are added to the solder paste as susceptors. The use of one or more inductively heatable susceptors which are built on or in a PCB is listed by patent in [11, 12]. However, real practical applications based on these are currently unknown.

## 2 Method for Induction Heating of PCB Assemblies

Methods for inductive heating can now be found in all sectors of industry. A special feature of inductive heating is that the heat is generated directly without contact in the workpiece. Furthermore, the energy density, which can be transmitted inductively, is much higher than it is possible with conventional heating methods. A classification of the inductive heating compared to other heating methods with regard to their power density is shown in Table 1.

In comparison to conventional heating methods which are used for soldering tasks (i.e. convection oven, vapor phase), inductive heating is characterized by a significantly higher energy efficiency.

**Table 1** Power densities of various heating methods [7]

| Heating method             | Power density [W/cm <sup>3</sup> ] |
|----------------------------|------------------------------------|
| Convection                 | 0.5                                |
| Radiation (muffle furnace) | 8                                  |
| Conduction (heat plate)    | 20                                 |
| Infrared heater            | 2 * 10 <sup>2</sup>                |
| Flame (burner)             | 10 <sup>3</sup>                    |
| Induction heating          | 10 <sup>4</sup>                    |
| Plasma jet                 | 10 <sup>6</sup>                    |
| Laser (CO <sub>2</sub> )   | 10 <sup>10</sup>                   |

### 2.1 Estimation of Loss Mechanisms within a Material

In order to determine the suitability of an electrically conductive material for the application presented here, it is necessary to be able to calculate the losses or their respective proportions. The equations used for this purpose are largely based on the works of Steinmetz [13], Jordan [14] and Bertotti [15]. The most comprehensive approach is provided by Bertotti in which he also takes into account the excess losses. The total losses ( $P_{Fe}$ ) result from the accumulation of hysteresis losses ( $P_h$ ), eddy current losses ( $P_e$ ) and excess losses ( $P_a$ ).

$$P_{Fe} = P_h + P_e + P_a \tag{1}$$

$$= k_h \cdot f \cdot \hat{B}^\beta + k_e (f \cdot \hat{B})^2 + k_a (f \cdot \hat{B})^{1.5}$$

The solution requires the material-specific coefficients  $k_h$ ,  $\beta$ ,  $k_e$  and  $k_a$ . Since these are not always available, they must be calculated. The simulation of the eddy current losses by means of FEM is comparatively easy to carry out. In this work, this was done with the software tool COMSOL Multiphysics 4.4. The determination of  $k_e$  can thus take place via the simulation. If ferromagnetic materials are to be quantified in addition to para- and diamagnetic materials, the coefficients for hysteresis and excess losses are also required. Since their simulation is far less trivial, they were calculated backwards from the total loss values often found in data sheets. Since there are three unknowns, the solution of Eq. (1) with three interpolation points is required. By way of example, this has been done here for a typical magnetic core material (20PNF1500 [16]). Fig. 4 shows the calculated loss shares of the material as a function of the frequency.

### 2.2 Requirements for Selective Heating of a PCB

In this work, solder joints are to be heated by means of general, non-specialized inductor geometries. A simple inductor form used here, was a cylindrical coil. A flat coil is another type of coil which could be used for induction heating. Flat coils can be designed meander shaped. For this case, however, the current directions of the individual windings are in opposite directions, as a result of which the field lines do not concentrate and a poor efficiency occurs. [7] For these studies, a spirally wound coil was used here, which has a comparatively high inductance. [7]

For the purpose of localized heating, specially designed susceptors are to be constructed in or on PCB's. These serve to couple in the magnetic field and constitute the heat source in the later soldering process.

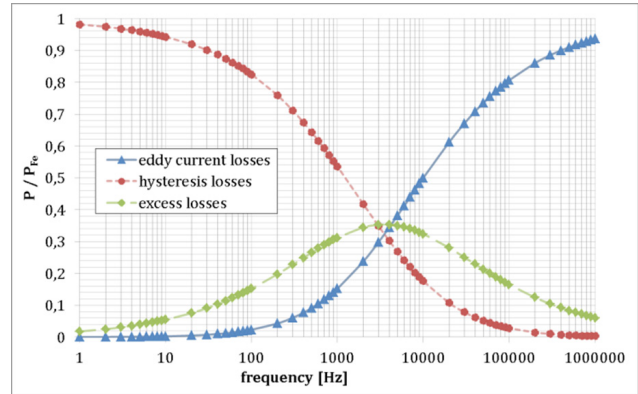


Fig. 4 Portion of individual loss mechanisms to the total magnetic core losses of the electrical steel 20PNF1500.

The geometry and material of these susceptors should be chosen in such a way that heating of the susceptor takes place, but not of the adjacent conductor tracks or components. For this purpose the skin effect is used, which generates a displacement of the induced eddy currents to the edge of the conductor geometry. Condition for a significant heating is that the dimensions of the conductor must be a multiple of the penetration depth  $\delta$ . [17]

$$\delta = \sqrt{\frac{1}{\sigma \cdot \pi \cdot f \cdot \mu}} \tag{2}$$

The dimensions of typical structures on PCBs (pads, conductor tracks) are in the mm-range in x-y-direction and in the double-digit  $\mu\text{m}$ -range in z-direction. The operating frequency ( $f$ ) of the inductor has to be chosen so low that no coupling of the magnetic field takes place in these structures anymore. Considering copper as the most common material on PCB's and taking Eq. (2) into account within the transverse magnetic field frequencies of up to 20 kHz are allowed. The penetration depth  $\delta_{Cu}$  here is 0.46 mm, so that structures  $< 1$  mm in width do not experience any distinct self-heating. In the longitudinal field, on the other hand, the thickness of the conductor tracks is crucial for coupling. Based on typical copper plating on assemblies, between 18 – 70  $\mu\text{m}$ , no frequencies higher than 100 kHz ( $\delta_{Cu} = 0.21$  mm) may be used here. Here, ferromagnetic materials are particularly suitable as susceptor materials since their penetration depths are much smaller due to their high permeabilities (i. e.:  $\delta_{Ni} = 0.017$  mm).

A graphical representation of different penetration depths in dependency of the frequency are depicted in Fig. 5. It should be noted, that the penetration depth is also dependent on the temperature. The electrical conductivity ( $\sigma$ ) as well as the relative permeability both change

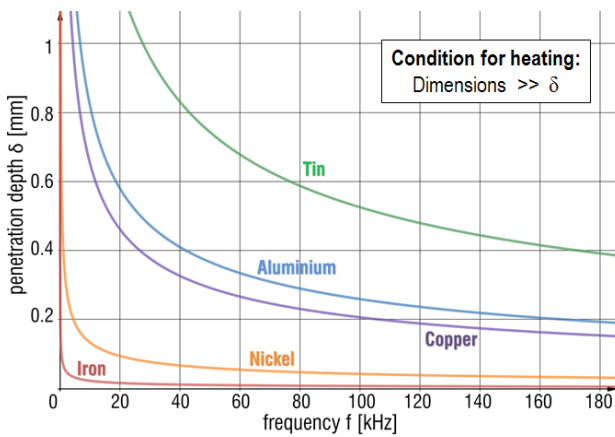


Fig. 5 Graph for the penetration depth in different materials depending on the frequency of the magnetic field.

with varying temperature. The conductivity for metals decreases for rising temperatures, which would result in an increased penetration depth at the same frequency. The temperature influence on the permeability depends strongly on the magnetic type as well as on the material itself. For example, with a ferromagnetic material the relative permeability decreases rapidly when its temperature is reaching the Curie point of the material.

### 3 Experimental

As already described, a distinction is made in this work between the inductive heating in the magnetic transverse field and the heating in the longitudinal magnetic field. The PCB samples are to be examined in a horizontal position and the susceptors installed therein usually have small  $z$  dimensions and larger  $x$ - $y$  dimensions. Therefore, in the transverse field the main component of the field strength is perpendicular to the susceptor and in the longitudinal field parallel to the susceptor.

For both methods, experimental setups with suitable inductor geometries were constructed or modified in order to heat PCB samples with susceptors attached to them. The selection of the susceptor materials was based (besides the availability) on the type of field and the respective working frequency. Exemplary soldering tests were carried out for both methods in order to demonstrate their general application.

#### 3.1 Experimental Setup for Induction

Commercially available inductive heating generators were tested for possible adaptation to the heating of electronic assemblies. The general buildup of a system for induction heating can be seen in Fig. 6. With regard

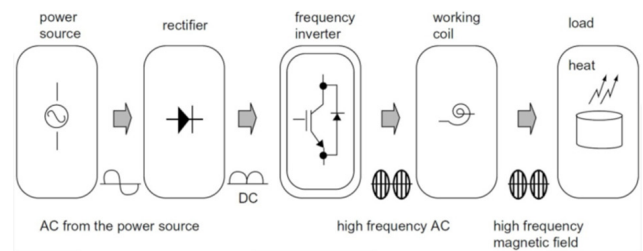


Fig. 6 Basic buildup of an induction heating system. [18, 19]

to the geometric requirements of printed circuit boards (load), a flat spiral working coil was used here at first. Furthermore, a way to control the generator power is useful. In addition, the lowest possible operating frequency is needed to minimize the risk of unwanted heating in the PCB or the components.

For heating in the inductive *transverse field*, the induction generator and the flat spiral coil of an industrial induction cooker (MKN type 203515) were converted. Its operating frequency is 20 kHz and the generator has an output power of 3.5 kW. The induction generator makes use of a series resonant half-bridge oscillator in a zero voltage mode with IGBT's as power switch. The basic circuit design of this oscillator type is depicted in Fig. 7.

Several modifications were necessary to adapt the cooking unit for the heating of small PCB Specimens. The cooking surface was removed and the exposed spiral coil was covered with a ceramic plate. This served as the area for sample holding, while not being susceptible to induction itself and also being stable against high temperatures. In addition, a new control unit with protection against overcurrent and overheating was realized. For safety reasons, such induction hobs can only be switched on if a sufficiently large secondary load is placed on the inductor (gen.: induction pots). At first, a large iron square was used here as a secondary load. Since this caused an asymmetrical distortion of the magnetic field, it was replaced in the following experiments by a symmetrical iron ring (outer part of a car brake disc). Fig. 8 shows the schematic of a PCB/susceptor specimen within the magnetic field of a flat coil inductor.

In order to investigate especially ferromagnetic susceptors, a test setup for heating in the *longitudinal magnetic field* was also designed. One possibility would have been to rotate appropriate samples by 90° and place them on the transverse field test stand. In this case, the main component of the magnetic field lines would run parallel to the susceptor surface. However, the flat coil used is unsuitable for such experiments due to its field geometry. This would

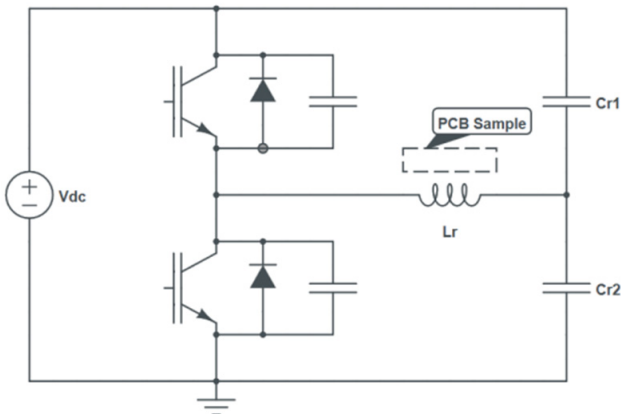


Fig. 7 Basic circuit of a half-bridge oscillator as main power source

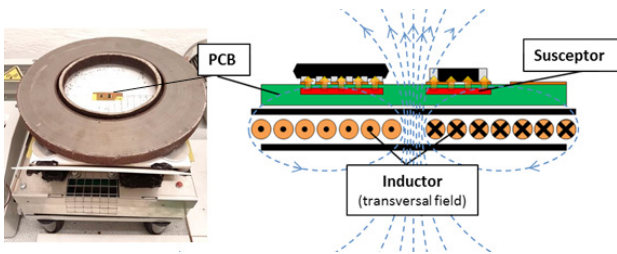


Fig. 8 Schema and setup of a PCB sample with susceptors in the magnetic field of a flat coil.

lead to a very irregular one-sided heating. Furthermore, the fixed operating frequency of the test stand of 20 kHz does not correspond to the required 100 kHz.

The test rig for longitudinal field heating should be used to investigate basic susceptor variants. Therefore, its construction should be as simple as possible. In order to achieve the required process temperatures for soldering later on, a power loss of approx. 20 W must occur within the susceptor. According to [7], efficiencies of up to 80 % can be achieved when heating ferromagnetic materials with appropriately adapted inductor coils. Therefore, the test stand was designed so that a laboratory power supply with 40 V / 5 A would be sufficient. The setup was executed as a self-oscillating variant based on a Royer-Converter (Fig. 9).

Due to the requirement to work at a resonance frequency ( $f_{res}$ ) of 100 kHz and with PCB samples of at least 20×20 mm in dimension, a self-wound cylindrical inductor was used. The desired frequency can be calculated by

$$f_{res} = \frac{1}{2\pi\sqrt{LC}} \quad (3)$$

where  $L$  is the inductivity of the inductor and  $C$  the capacity of the resonant circuit. The self-wound coil had a length

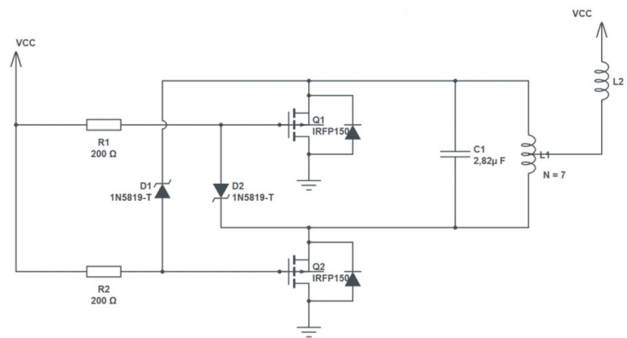


Fig. 9 Circuit diagram of a self-oscillating Royer-Converter

of  $l = 35$  mm, a diameter of  $d = 30$  mm and was wound  $N = 7$  times. As an approximation, the equation

$$L = \frac{\mu N^2 \pi d^2}{4l} \quad (4)$$

can be used, which results in an inductance of about 1 μH. With Eq. (4) the total capacity could be set to  $C = 2.82$  μF. The inductor material was copper and it was designed as a hollow conductor. Therefore it could simply be water-cooled during operation. Since the entire test setup was kept quite compact, the cooling also provided for heat dissipation at the capacitor bank, which allowed for longer test times before overheating would occur. Fig. 10 shows the schematic of a PCB/susceptor specimen within the magnetic field of a cylindrical coil inductor.

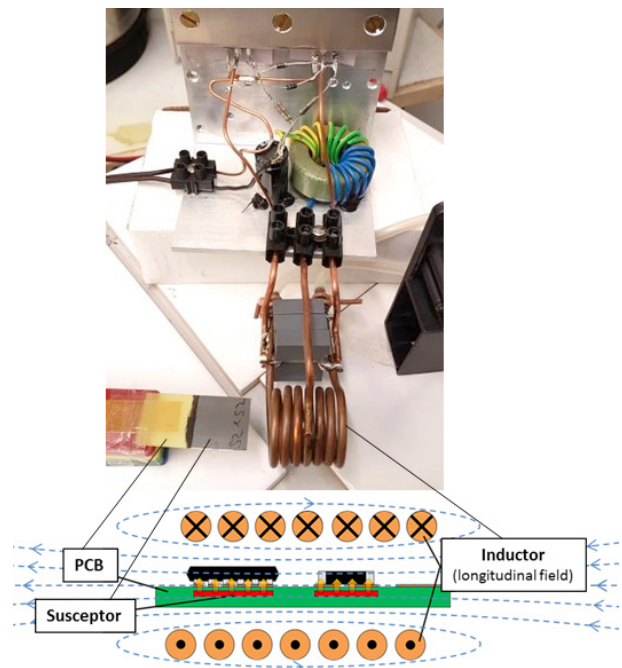


Fig. 10 Schema and setup of a PCB sample with susceptors in the magnetic field of a cylindrical coil.

### 3.2 Experimental setup for Demo Soldering

After constructing the test stands and examining suitable susceptor materials for both field geometries, a fundamental experiment should demonstrate the feasibility of reflow soldering with inductive heating. For this purpose, small test boards (Fig. 11) made of epoxy or polyimide substrate material were designed. As demo components an inverter (LS04) and a voltage regulator (LM78L12ACM) were chosen. The selection was made for reasons of easy testability of both components after the soldering process in the induction field.

As indicated in Fig. 11, for the sake of simplicity, the susceptors were positioned on the back. From a thermal point of view, this is of course a more lossy structure than when the susceptor rests inside the circuit board. In order to achieve a low thermal resistance between the solder on the top, substrates of thickness 0.25 mm were used.

The susceptor size was 20×30 mm. For the experiments in the transverse field, copper susceptors with a thickness of 100 μm were chosen. When soldering in the longitudinal field, galvanically constructed nickel susceptors with a layer thickness of approx. 60 μm are most suitable.

For automatic process control of the soldering tests, a control loop was set up and a control software was designed using LabVIEW. Due to the different hardware and the different measurement options, the control loops differ for transverse and longitudinal field tests. Thus, for example, in the transverse field, the temperature measurement can be performed by means of a pyrometer or IR (infrared) camera. Fig. 12 shows the control circuit used for the soldering tests in the magnetic transverse field.

The structure of the longitudinal field control can be seen in Fig. 13. Here the use of IR devices were not possible hence the optical blocking by the coil. Instead a temperature dependent resistor was mounted and used for the thermal measurement.

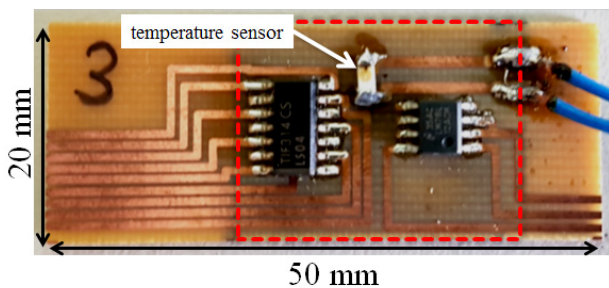


Fig. 11 Specimen for inductive soldering test with susceptor (dashed area) on the backside.

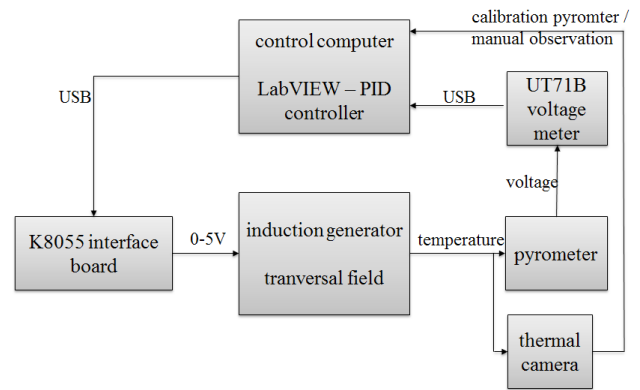


Fig. 12 Control circuit for automatic process control of induction soldering tests in the transversal field.

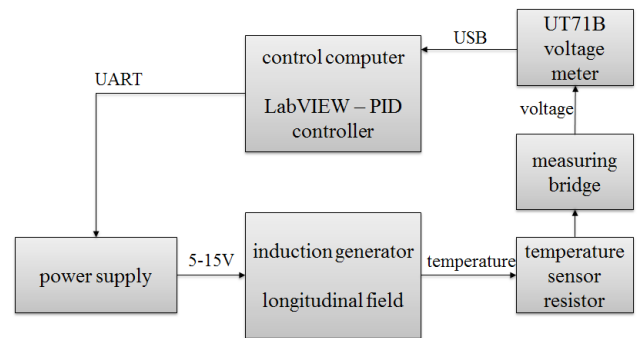


Fig. 13 Control circuit for automatic process control of induction soldering tests in the longitudinal field.

## 4 Results

### 4.1 Susceptor Materials within the Induction Setups

In these investigations a wide variety of metallic materials were examined for their suitability as susceptor materials. First, it was important to ensure that the materials were available and can be integrated into PCB's with standard technology. In addition, only the susceptors in each respective field geometry should heat up and not the other metallic components on a PCB.

For the transverse field heating mainly diamagnetic copper and paramagnetic aluminum in the form of sheets and foils were used. Copper susceptors can be made directly from the PCB plating. Fig. 14 a) shows such a susceptor on the backside of a sample for soldering. In addition to the electrical conductivity, especially the geometric dimensions influence the induction in the material. Due to the limited field homogeneity in the center of the inductor, x-y dimensions of approximately 20×20 mm have proven to be suitable. But also the susceptor thickness has an influence here because it changes the electrical resistance against induced eddy currents. An FEM calculation resulted in

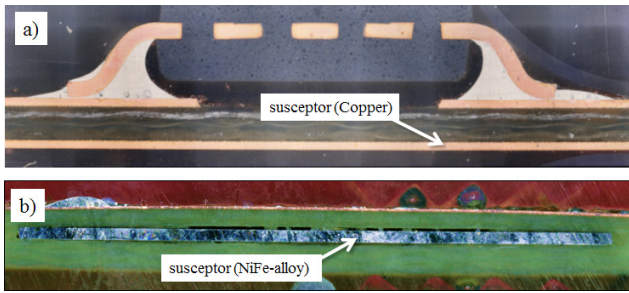


**Fig. 14** Cross section of PCB samples with a susceptor made of a) copper and b) NiFe-alloy (Permenorm®).

an optimum thickness of 100  $\mu\text{m}$  for copper on our setup, since this is where the point of adaptation is achieved. For aluminum, the simulated optimum was around 80  $\mu\text{m}$ .

Ferromagnetic materials are only partially suitable for the transverse field heating. Since these direct the magnetic flux, which leads to mix of longitudinal and transverse field heating within the inductor middle. The result is a lower power loss. However, as already described, ferromagnetics have a much smaller penetration depth and are therefore suitable for longitudinal field heating in which they allow a small thickness in combination with PCB substrates.

The investigation at the cylinder inductor were mainly conducted with thin sheets (50–200  $\mu\text{m}$ ) of various Nickel-Iron-alloys like Permenorm® (36%Ni-64%Fe), Ultravac® (44%Ni-3%Mo-53%Fe) and permalloy (81%Ni-19%Fe). Furthermore, galvanically deposited layers ( $\sim 100\mu\text{m}$ ) of iron and nickel as well as specially mixed ferrite pastes with iron, nickel or magnetite ( $\text{Fe}_3\text{O}_4$ ) powder were used. Above all, nickel is interesting because it is already used technologically in the printed circuit board industry. When creating the pastes, the highest possible degree of filling was used to maximize the power loss. In the induction experiments, it has been shown that the heating is predominantly due to hysteresis- and excess losses, since eddy currents rarely occur in the separated material particles ( $\varnothing_{\text{Ni}} \approx 2.5 \mu\text{m} / \varnothing_{\text{Fe}} \approx 5\text{-}15 \mu\text{m}$ ) or due to the weak conductivity of the iron oxide can.

#### 4.2 Demo Soldering Test

An IR camera was used primarily for monitoring and assessing the temperature distribution. An example of the IR radiation during a soldering process in the transverse field is shown in Fig. 15.

In the cylindrical inductor, the optical temperature measurement through the barrier of the inductor winding is not possible. Here, instead, calibrated electrical resistors

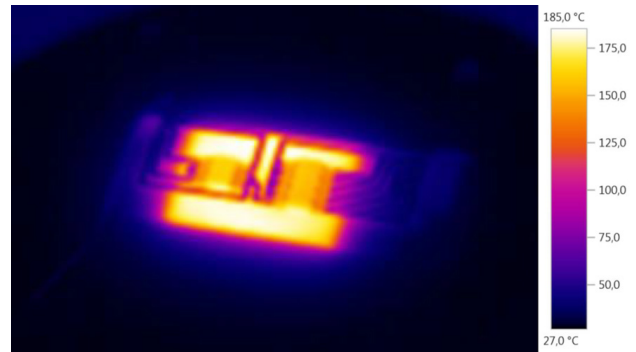


**Fig. 15** Temperature radiation ( $\epsilon = 0.97$ ) of a pcb sample during a soldering test in the induction field.

were used, which were previously fixed with a high temperature solder (Pb93Sn5Ag2). The use of the usual thermocouples (Type-K) is not advisable, since it can lead to interference in the wires by the magnetic field.

To demonstrate the solderability in the different induction fields corresponding soldering profiles were set. These are based on standard convection reflow profiles and on the solder alloy used (Sn96.5Ag3Cu0.5). Fig. 16 shows the soldering profiles used depending on the field geometry. In the 60  $\mu\text{m}$  thin nickel susceptor only a part of the power could be converted at maximum load, therefore the heating time in the peak zone is significantly longer. The profile for the longitudinal field had to be designed somewhat longer compared to the transverse field. In its current version, the temperature control tends to overshoot, which may result in slightly higher temperatures at the sample than specified.

Soldering tests were successfully carried out at both test stands. In a subsequent functional test on the components used, no errors could be determined. While the polyimide base material had undergone all tests unscathed, a slight

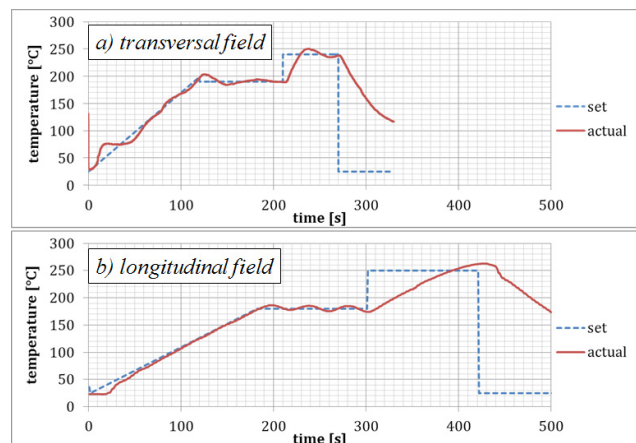


**Fig. 16** Temperature profiles for soldering within induction fields.

discoloration in the area of the susceptor could be found on the epoxy material.

A metallographic analysis of selected solder joints revealed a high number of voids in the viewed solder joint cross-sections. (Fig. 17) Their occurrence can have many reasons. For once, in some of the samples, the solder paste deposits had to be applied manually to the pad because stencil printing was not possible. Hereby, the amount of paste volume can vary. Larger volumes are more likely to produce voids. In addition, standard solder pastes for convection soldering were used here whose flux systems are not adjusted and optimized for the temperature gradients and hold times of this inductive soldering process.

### 4.3 Electrical Components in the Induction Field

A point that is equally critical for both fields of induction is the possibility of coupling in certain components, resulting in thermal or electrical faults and even destruction. Most passive SMT components are too small in size to cause significant heating. Especially larger components like inductors or e-caps exhibited a significant self-heating during induction tests. For example, an electrolytic capacitor in radial design with 47 $\mu$ F and a housing dimension of 10 $\times$ 20 mm, developed a self-heating of about 180 °C after 60 s.

For ICs, the tendency to self-heating depends on the respective lead frame material. Ferromagnetic frames like Alloy 42 or Kovar<sup>®</sup> are considered to be particularly critical here. Fig. 18 depicts such a lead frame and its heating (up to 100°C) within a magnetic field.

### 5 Conclusion

Within this study, two different inductive heating methods could be investigated regarding their suitability for soldering processes. An advantage of the transverse field heating lies in the production of susceptors which could be made from the copper on a PCB. Furthermore, susceptors are heated solely by induced eddy currents. This simplifies the simulation or prediction of behaviors during the heating process. Disadvantages of this induction variant arise from the design limitations of the PCB layout. At the operating frequency of 20 kHz selected here, conductor tracks must not become wider than 2 mm. The susceptor, however, must have an edge length of min. 20 mm. Higher frequencies would allow for smaller susceptors, but the conductor tracks would have to be narrowed in the same

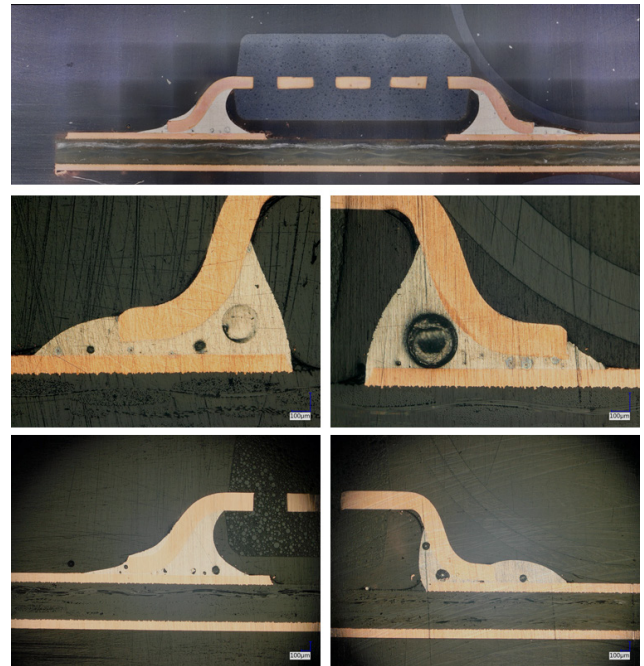


Fig. 17 Metallographic cross-sections of selected solder joints produced via induction soldering.

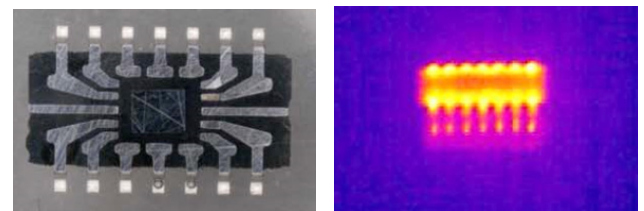


Fig. 18 Cross-section (l.) of an IC with a ferromagnetic lead frame and its heating inside a magnetic field (r.).

ratio. Also the formation of closed conductor loops in the design must have to be avoided. Another critical point of this heating method is the inhomogeneity of the magnet field generated by flat coils, which leads to an irregular heating of large susceptors or susceptor assemblies. Also, a single large inductor appears unsuitable for a continuous production processes.

The heating in the longitudinal magnetic field shows its strength in the efficiency. In order to prevent heating, in this method, the conductor geometry is limited in its height instead its width. The formation of conductor loops is not important. Further advantages are the suitability of the method for continuous processes due to the use of circulating inductors and the uniform temperature distribution in the susceptor.

## References

- [1] Géczy, A., Illés, B., Illyefalvi-Vitéz, Z. "Modeling method of heat transfer during Vapour Phase Soldering based on filmwise condensation theory", *International Journal of Heat and Mass Transfer*, 67, pp. 1145–1150, 2013.  
<https://doi.org/10.1016/j.ijheatmasstransfer.2013.08.072>
- [2] Seehase, D., Huth, H., Bremerkamp, F., Nowottnick, M. "Energetic Analysis of Solder Paste Deposits as Reference for Soldering with Selective Heat", In: 2012 35th International Spring Seminar on Electronics Technology, Bad Aussee, Austria, 2012, pp. 31–36.  
<https://doi.org/10.1109/ISSE.2012.6273103>
- [3] Seehase, D., Lange, F., Novikov, A., Nowottnick, M. "Material Study for full-faced Heating Layers, integrated in Printed Circuit Boards", In: 2017 40th International Spring Seminar on Electronics Technology (ISSE), Sofia, Bulgaria, 2017, pp. 1–6.  
<https://doi.org/10.1109/ISSE.2017.8000898>
- [4] Seehase, D., Novikov, A., Nowottnick, M. "Resistance Development on Embedded Heating Layers during Climatic Test", In: 2017 21st European Microelectronics and Packaging Conference (EMPC) & Exhibition, Warsaw, Poland, 2017, pp. 1–5.  
<https://doi.org/10.23919/EMPC.2017.8346909>
- [5] Seehase, D., Neiser, A., Lange, F., Novikov, A., Nowottnick, M. "Thermal Characterization of Endogenously Heated Printed Circuit Boards with Embedded Resistive Layers", In: 7th Electronics System-Integration Technology Conference, Dresden, Germany, 2018, pp. 1–9.
- [6] Zhang, Y., Cheng, M., Pillay, P. "Magnetic Characteristics and Excess Eddy Current Losses", In: 2009 IEEE Industry Applications Society Annual Meeting, Houston, TX, USA, 2009, pp. 1–5.  
<https://doi.org/10.1109/IAS.2009.5324814>
- [7] Peter, H.-J. "Handbuch induktives Löten" (Manual Inductive Soldering), Peter Verlag, Berlin, 2014. (in German)
- [8] Wolf, E. "Weichlöten mit Induktionserwärmung" (Soldering with Induction Heating), *productronic*, 10, pp. 2–4, 2003. (in German)
- [9] Li, M., Xu, H., Lee, S. R., Kim, J., Kim, D. "Eddy Current Induced Heating for the Solder Reflow of Area Array Packages", *IEEE Transactions on Advanced Packaging*, 31(2), pp. 399–403, 2008.  
<https://doi.org/10.1109/TADVP.2008.923385>
- [10] Habib, A. H., Ondeck, M. G., Miller, K. J., Swaminathan, R., McHenry, M. E. "Novel Solder-Magnetic Particle Composites and Their Reflow Using AC Magnetic Fields", *IEEE Transactions on Magnetics*, 46(6), pp. 2187–2190, 2010.  
<https://doi.org/10.1109/TMAG.2010.2044640>
- [11] Iriguchi, S., Hatanaka, K., Watanabe, S., Taketomi, N., Yamamoto, K., Sugie, M., Fujitsu Ltd "Method of repair of electronic device and repair system", U.S. Patent Nr. 8,456,854, 2013.
- [12] Chan, H. A., Oien, M. A., Nokia Bell Labs "Localized Soldering by Inductive Heating", U.S. Patent Nr. 4,983,804, 1989.
- [13] Steinmetz, C. P. "On the law of hysteresis", *Proceedings of the IEEE*, 72(2), pp. 197–221, 1984.  
<https://doi.org/10.1109/PROC.1984.12842>
- [14] Jordan, H. "Die ferromagnetischen Konstanten für schwache Wechselfelder" (The ferromagnetic constants for weak alternating fields), *Elektrische Nachrichten Technik*, 1, 1924. (in German)
- [15] Bertotti, G. "General properties of power losses in soft ferromagnetic materials", *IEEE Transactions on Magnetics*, 24(1), pp. 621–630, 1998.  
<https://doi.org/10.1109/20.43994>
- [16] Posco "Electrical Steel", data sheet, 2014.
- [17] Marinescu, M. "Elektrische und magnetische Felder. Eine praxisorientierte Einführung" (Electric and magnetic fields. A practice-oriented introduction), Springer Verlag, Berlin, 2012. (in German)  
<https://doi.org/10.1007/978-3-540-89697-5>
- [18] Zinn, S., Semiatin, S. L. "Elements of Induction Heating: Design, Control, and Applications", ASM International, Metals Park, Ohio, USA, 1988.
- [19] Semiconductor Components Industries, LLC "AN-9012 - Induction Heating System Topology Review", 2013, [online] Available at: [www.fairchildsemi.com](http://www.fairchildsemi.com) [Accessed: 02 November 2018]